Journal of Medicinal Chemistry Article

J. Med. Chem. **2010,** *53,* 4379–4389 **4379**
DOI: 10.1021/jm901692q

Novel Alpha-7 Nicotinic Acetylcholine Receptor Agonists Containing a Urea Moiety: Identification and Characterization of the Potent, Selective, and Orally Efficacious Agonist 1-[6-(4-Fluorophenyl)pyridin-3-yl]-3-(4-piperidin-1-ylbutyl) Urea (SEN34625/WYE-103914)

Chiara Ghiron,*[,†,§] Simon N. Haydar,[‡,§] Suzan Aschmies,[‡] Hendrick Bothmann,[†] Cristiana Castaldo,[†] Giuseppe Cocconcelli,[†] Thomas A. Comery,[‡] Li Di,[‡] John Dunlop,[‡] Tim Lock,[‡] Angela Kramer,[‡] Dianne Kowal,[‡] Flora Jow,[‡] Steve Grauer,[‡] Boyd Harrison,[‡] Salvatore La Rosa,[†] Laura Maccari,[†] Karen L. Marquis,[‡] Iolanda Micco,[†] Arianna Nencini,[†] Joanna Quinn,[†] Albert J. Robichaud,[‡] Renza Roncarati,[†] Carla Scali,[†] Georg C. Terstappen,[†] Elisa Turlizzi,[†] Michela Valacchi,[†] Maurizio Varrone,[†] Riccardo Zanaletti,[†] and Ugo Zanelli[†]

[†]*Siena Biotech SpA, Strada del Petriccio e Belriguardo 35, 53100 Siena, Italy, and* [‡]*Chemical Sciences and Neuroscience Discovery Research, Wyeth Research, CN 8000, Princeton, New Jersey 08543-8000.* [§]*These authors contributed equally to this work.*

Received November 16, 2009

Alpha-7 nicotinic acetylcholine receptor (α7 nAChR) agonists are promising therapeutic candidates for the treatment of cognitive impairment. We report a series of novel, potent small molecule agonists (**4**−**18**) of the α7 nAChR deriving from our continuing efforts in the areas of Alzheimer's disease and schizophrenia. One of the compounds of the series containing a urea moiety (**16**) was further shown to be a selective agonist of the α7 nAChR with excellent in vitro and in vivo profiles, brain penetration, and oral bioavailability and demonstrated in vivo efficacy in multiple behavioral cognition models. Structural modifications leading to the improved selectivity profile and the biological evaluation of this series of compounds are discussed.

Introduction

Cognitive disorders encompass a wide range of diseases and represent a still unmet medical need in the psychiatric and neurology therapeutic area. In particular, the negative symptomatology (cognitive impairments, reduced affect, social withdrawal, low motivation) of schizophrenia is largely unaffected by current antipsychotic medications that block dopamine D2 receptors, and in Alzheimer's disease, the most common form of dementia, only modest symptomatic improvement in cognitive performance is provided by standard of care agents such as acetyl cholinesterase inhibitors and 3,5-dimethyladamantan-1-ylamine (memantine, a NMDA[a] receptor antagonist).

Several lines of experimental evidence support the involvement of the neuronal nicotinic receptors in both schizophrenia and AD.[1−4] These include reduced expression of α7 nicotinic acetylcholine receptors (nAChR) in brain tissue from schizophrenia and AD patients, as well as genetic linkage studies in schizophrenia, implicating the locus of the α7 receptor gene promoter.[5] Prototypical α7 receptor agonists have demonstrated improved cognition in animal models and normalized sensory gating deficits, which are believed to contribute to the cognitive fragmentation in schizophrenia.[6,7] On the basis of these observations, there is strong hope that selective α7 nAChR agonists will prove effective in the improvement of cognition in both schizophrenia and AD.[8−10] In accordance with this hypothesis, the prototypical nAChR agonist nicotine, as well as more selective α7 agonists such as 2-methyl-5-[6-phenylpyridazin-3-yl]octahydropyrrolo[3,4-*c*]pyrrole (A-582941) described recently, have been shown to improve cognitive performance in both animal models and human clinical trials.[11]

As part of a multidisciplinary approach toward the treatment of schizophrenia and Alzheimer's disease, a medicinal chemistry project was initiated to develop selective α7 agonists. In the initial phase of the program, structure−activity relationship work around the initial amide "hit" *N*-{4-[4-(2,4-dimethoxyphenyl)-piperazin-1-yl]butyl}-4-pyridin-2-ylbenzamide (**1**, Figure 1)[12] allowed the identification of the agonist "lead" 5-morpholin-4-yl-pentanoic acid (4-pyridin-3-yl-phenyl)-amide SEN12333/WAY-317538[13,14] (**2**, Figure 1).

Although displaying only moderate potency against the α7 nicotinic receptor (EC_{50} = 1.65 μM), "reverse amide" **2** showed promising overall selectivity and pharmacokinetic profiles, displayed in vivo activity in various animal models and was deemed worthy of further optimization. Starting from **2**, medicinal chemistry efforts were focused to further improve both the potency and the selectivity from the initial

*To whom correspondence should be addressed. Phone: (+39) 0577381408. Fax: (+39) 0577381303. E-mail: cghiron@sienabiotech.it.

[a]Abbreviations: ACh, acetylcholine; AChBP, acetylcholine binding protein, AD, Alzheimer's disease; AMMC, 3-[2-(*N*,*N*-diethyl-*N*-methylamino)ethyl]-7-methoxy-4-methylcoumarin; BFC, 7-benzyloxy-4-trifluoromethylcoumarin; ACN, acetonitrile; CHO, Chinese hamster ovary; DCM, dichloromethane; ES, electrospray; FA, formic acid; FLIPR, fluorescence imaging plate reader; HBSS, Hank's balanced salt solution; HEK, human embryo kidney; hERG, human ether-a-go-go-related gene; HPLC-MS, high pressure liquid chromatography−mass spectrometry; HR-MS, high resolution mass spectrometry; HTS, high-throughput screening; LTQ, linear trap quadrupole; MED, minimum efficacious dose; MFC, 7-methoxy-4-trifluoromethylcoumarin; NMDA, *N*-methyl-D-aspartate; NOR, novel object recognition; P450, cytochrome P450; PAMPA, parallel artificial membrane permeability assay; PDA, photodiode array; PPI, prepulse inhibition; SAR, structure−activity relationship; SCX, strong cation exchanger; TLC, thin layer chromatography; TOF, time-of-flight; UPLC, ultra performance liquid chromatography.

Published on Web 05/14/2010

series. Molecular modeling studies were also applied to investigate the structural basis of ligand−receptor binding and to define the pharmacophoric features of described α7 agonists. Herein we report the synthesis and SAR of novel derivatives which are potent and selective agonists of the α7 nAChR.

Results and Discussion

During the initial phase of structure−activity exploration on the amide series, we noticed that the basicity of the left-hand side amine was crucial to the modulation of potency at the α7 receptor.[13] The presence of a more basic amine was usually associated with higher potency. This can be related to stronger cation−π interactions, reportedly[15] important in the ligand−receptor association.

We chose piperidine as the "reference" amine around which to explore further structural variations as piperidine was found to confer a minimal potency level (compare for example compound **3** to morpholine-containing **2** in Table 1), thus facilitating the impact of modifications in other areas of the molecules. Similarly, we previously found that the presence of a pyridine ring in the right-hand side biaryl system was beneficial, so we initially kept this feature unchanged.[13]

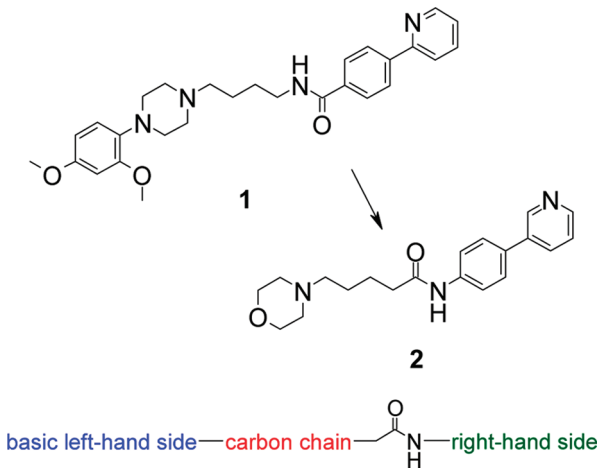

Figure 1. Initial hit (**1**) and lead (**2**) molecules, with schematic pharmacophore features.

For the present study, we decided to primarily explore a carbon chain length of four carbon atoms. Having observed that increasing the chain length to five carbons resulted in only small functional potency changes (Table 1, compounds **3** and **4**), we investigated the impact of replacing the amide moiety with a urea in the four-carbon chain series. We noted that potency in the urea series was maintained if not improved (Table 1, compare results for compounds **4** and **5**). This can at least in part be explained by assuming the urea derivatives to be a "combination" of the initial amide hit series (as represented by **1**) and the longer chain "reverse amides" series to which lead molecule **2** belongs. We were also pleased to see that amine basicity impacted on potency with the same general trend (Table 1, compare results for compounds **5** and **6** to **3** and **2**, respectively), thus confirming this part of the SAR.

The α7 receptor comprises five homologous subunits, each consisting of extracellular and transmembrane main domains.[18] Although the α7 X-ray crystal structure has not been determined to date, several crystals of α7 agonists bound to the extracellular domain of the homologous acetylcholine binding protein (AChBP) are available[19] and commonly used as templates to build homology models. The agonist binding site is located at the interface between two adjacent subunits in the extracellular domain of the receptor and is mainly defined by an aromatic cage composed of W53, Y89, W143, Y164, and Y185 and a disulfide-bridged loop (Cys-loop). Cation−π or hydrogen bond interaction to W143 are reported to be key pharmacophoric features for α7 agonists.[20] To determine the structural components of the urea series potentially responsible for the biological activity observed, we applied molecular modeling methods, docking representative compounds into the orthosteric binding site of a human α7 homology model.

In the putative binding mode of compound **5** into the theoretical model for human α7 receptor, the protonated nitrogen of piperidine makes hydrogen bond contact to the backbone carbonyl of W143. The urea moiety is placed within

Table 1. Effect of the Amine Basicity, Chain Length, and Amide Moiety Replacement on Activity[16]

Compound	Structure	α7 EC_{50} (μM) ± SEM (n)[a]
2	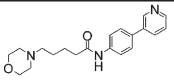	1.65 ± 0.43 (4)
3	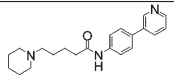	0.35 ± 0.17 (2)
4	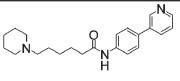	0.89 ± 0.08 (2)
5	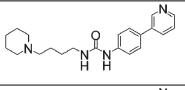	0.12 ± 0.02 (2)
6	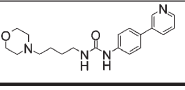	0.49 ± 0.08 (3)

[a] All functional activities were measured in a calcium flux assay using a fluorescence imaging plate reader. Activity at rat α7-nAChRs was determined using a stable recombinant GH4C1 cell line expressing the receptor.[17] Reported EC_{50}/IC_{50} values were determined in a single experiment and obtained from triplicate data points generated within the same experimental session. Data are averaged from multiple experiments (n) and reported as the average ± SEM (n). Nicotine under the same conditions had EC_{50} = 1.34 μM ± 0.02 (n = 62). Compounds with E_{max} > 70% of nicotine were considered to be full agonists. All reported compounds gave values >90%.

the aromatic cage, with the delocalized electronic system stacking over Y89 (Figure 2). The four-carbon chain serves as spacer between the piperidine and the urea pharmacophoric centers. In our studies, the right-hand side biaryl system appears to reach an area of the agonist binding site rich in hydrophilic residues (highlighted in blue in Figure 2), making this region prone to hydrogen bonding contacts to the pyridine nitrogen of compound **5**.

With this information in hand, and considering that a urea moiety would be intrinsically more stable than an amide, we set out to explore the urea class in more detail. A representative selection of the molecules which were synthesized is shown in Table 2 with their α7 activity, selectivity over homologous receptor subtypes, and early profiling data. The selection of Table 2 aims to explore the effects of ring substitution in terms of steric hindrance and torsional angle of the biaryl system and electronic effects on the aromatic rings. In our selection of substituents, we selected moieties that would allow for further exploration of the hydrophilic region pointed out by the docking studies without introducing additional hydrogen-bond donors beyond the ones brought by the urea linker itself to avoid increasing the polar surface area and thus potentially depressing brain penetration.[21]

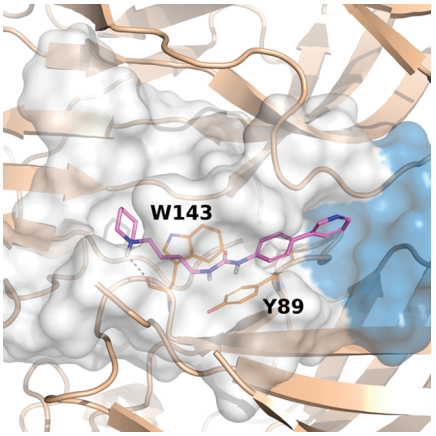

Figure 2. Compound **5** docked into the orthosteric site of the homology model for human α7 nAChR. Residues involved in key interactions with the ligand are highlighted in orange. For sake of clarity, part of the Cys-loop has been removed from the image. Amino acid numbering refers to the 1UW6 sequence which X-ray structure was used as a template for homology modeling.

As can be observed from the data reported in Table 2, all compounds maintained an excellent level of activity including unsubstituted compound **7**, showing a relative breadth of modifications possible for the second aryl ring and demonstrating the impact of the urea moiety on receptor affinity. With the exception of **10**, solubility and passive permeability were also excellent, showing potential for further progression.

Although no clear indications of a strong SAR was obtained with regards to α7 potency, all compounds with the exception of **12** presented relatively high activity against the homologous ganglionic receptor (α3) as well as substantial cytochrome P450 inhibition, especially the 2D6 subtype. Considering that SAR analysis takes into account the impact of modifications on the main target of interest as well as the effects on the overall compound profile, we favored those substituents showing an acceptable balance of properties.

Given that the presence of a pyridyl ring appeared to improve selectivity against α3 (compound **12**) and to lower 2D6 inhibition (compound **11** and **12**), and that lipophilicity tends to be one of the major factors in molecular recognition by the cytochrome family of enzymes,[24] we prepared a number of analogues where pyridine replaced the first phenyl ring of the right-hand side biaryl system. We maintained the pyridine nitrogen potentially pointing to the same binding area as in compound **12**, hoping that the reasons for the observed improvement in selectivity could be the result of unfavorable interactions with the α3 receptor. Results are reported in Table 3, where compounds **13**−**18** are exact analogues of **7**−**12**, respectively.

While again with almost no exceptions the molecules showed excellent solubility, passive diffusion permeability, and metabolic stability, we were pleased to see that their profile in terms of selectivity was further improved over the

Table 2. Activity, Selectivity (EC_{50} for Agonist Behavior, IC_{50} for Antagonist Behavior, μM), Solubility (Sol, μM), Permeability Class (Perm), Metabolic Stability (Met Stab, % Remaining), P450 Subtype Percent Inhibition at 3 μM, for a Representative Selection of Phenyl Urea Derivatives

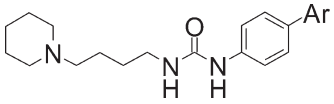

Cpd	Ar	Activity[a] (EC_{50}) α7	Selectivity[a] (IC_{50}) α1	α3	5HT3	Sol[b]	Perm[c]	Met Stab[d]	P450 Inhibition[e] 2D6	3A4	2C9
7		0.26±0.05 (2)	>30	2.8	7.9	108	High	100	64	51	2
8		0.14±0.03 (2)	7.7	1.1	7.8	114	High	100	38	5	-2
9		0.13±0.03 (3)	8.2	1.2	5.7	95	High	88	75	-17	-1
10		0.22 ± 0.003 (2)	8.0	1.7	5.8	20	Low	100	65	-13	-16
11		0.12 ± 0.01 (2)	>30	1.2	>30	158	High	100	21	-22	-18
12		0.13±0.01 (2)	>30	5.0	>30	153	High	97	15	-2	0

[a]All functional activities were measured in either calcium flux or membrane potential assays using a fluorescence imaging plate reader. Compounds with E_{max} > 70% of nicotine were considered to be full agonists. The reported compounds gave values > 90%. [b] Solubilities were determined at pH 7.4 at pseudothermodynamic equilibrium. [c] Permeability is based on measuring the permeation rate of the test article through an artificial membrane. The assay uses a mixture of porcine pig brain lipids in dodecane (2% w/v).[22] [d] Metabolic stability was determined as percentage remaining after incubation for 1 h with recombinant hCYP3A4. [e] Percent cytochrome inhibition[23] values < 15−20% were considered low. See Experimental Section for further details on all assays.

Table 3. Activity, Selectivity (EC_{50} for Agonist Behavior, IC_{50} for Antagonist Behavior, μM), Solubility (Sol, μM), Permeability Class (Perm), Metabolic Stability (Met Stab, % Remaining), P450 Subtype Percent Inhibition at 3 μM, for a Representative Selection of Pyridyl Urea Derivatives[a]

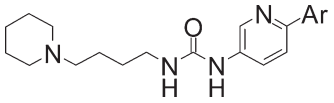

Cpd	Ar	Activity (EC_{50}) α7	Selectivity (IC_{50}) α1	α3	5HT3	Sol	Perm	Met Stab	P450 Inhibition 2D6	3A4	2C9
13		0.12±0.03 (2)	>30	10.1	>30	193	High	100	6	-21	-4
14		0.23±0.03 (2)	>30	3.9	>30	174	High	88	8	8	6
15		0.15±0.04 (2)	>30	5.6	>30	196	High	100	14	-3	-10
16		0.07±0.01 (16)	15.1	7.3	>30	121	High	75	19	0	-17
17		0.53 ± 0.19 (2)	>30	> 30	>30	205	High	100	8	-19	-10
18		0.39 ± 0.19 (2)	>30	9.88	>30	171	Medium	100	22	0	-3

[a] Notes as in Table 2: All functional activities were measured in either calcium flux or membrane potential assays using a fluorescence imaging plate reader. Compounds with E_{max} > 70% of nicotine were considered to be full agonists. The reported compounds gave values >90%. Solubilities were determined at pH 7.4 at pseudothermodynamic equilibrium. Permeability is based on measuring the permeation rate of the test article through an artificial membrane. The assay uses a mixture of porcine pig brain lipids in dodecane (2% w/v).[22] Metabolic stability was determined as percentage remaining after incubation for 1 h with recombinant hCYP3A4. Percent cytochrome inhibition[23] values <15−20% were considered low. See Experimental Section for further details on all assays.

Table 4. Pharmacological Characterization and Rat PK Parameters for Compound **16**

additional pharmacology	α7 K_i (nM)	44
	α7 e-phys[a] EC_{50} (nM)	490
	α7 e-phys[a] E_{max} (%)	70
	α4β2 IC_{50},EC_{50} (μM)	>30
	hERG[b] IC_{50} (μM)	1.3
PK	C_{max} (ng/mL)[c]	40
	T_{max} (h) [c]	5.3
	AUC_{last} (h·ng/mL) [c]	318
	%F[d]	100
	B/P[e]	0.3

[a] Whole cell patch clamp recordings were performed on GH4C1 cells expressing rat α7 receptors. Each cell was exposed to at least one concentration of acetylcholine and a full range of concentrations of **16**. [b] hERG response was obtained from CHO cells stably expressing the channel using an IonWorks system. [c] Pharmacokinetic parameters were determined following a single 3 mg/kg po dose in male Long Evans rats. [d] Oral bioavailability (%F) was determined in a separate experiment as the ratio of AUC_{0-inf} normalized for the dose, obtained following single 2 mg/kg iv and 10 mg/kg po doses in male Han Wistar rats. In the same experiment, the determined $T_{1/2}$ was 3.5 h. [e] The brain to plasma (B/P) ratio was determined as the ratio of $AUC_{0\text{-}inf}$ following a single 2 mg/kg po dose in male Han Wistar rats. In this experiment, AUC_{0-inf} for plasma and brain were 768 and 215 h·ng/mL, respectively.

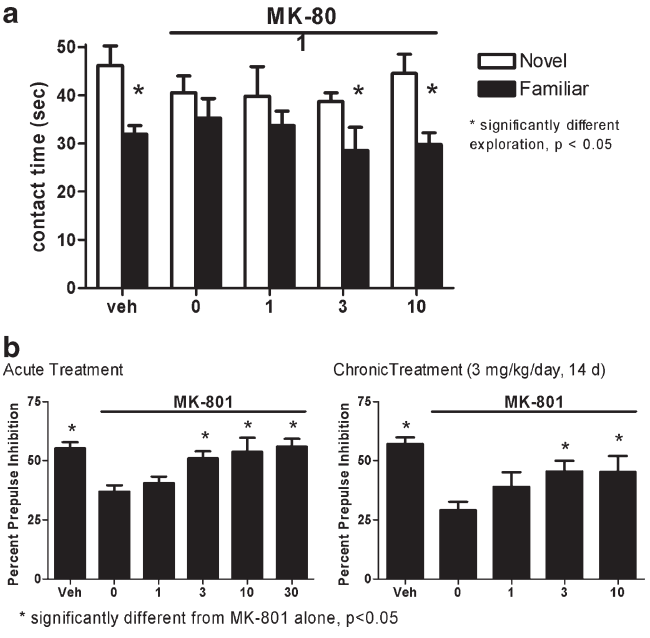

Figure 3. (a) In vivo results for compound **16**. MK-801-induced deficit in the novel object recognition test. Compound **16** blocks the MK-801-induced deficit in the novel object recognition test (1 h delay) in Long Evans rats. (b) In vivo results for compound **16**. MK-801-disrupted prepulse inhibition test. Compound 16 blocks the MK-801-disrupted prepulse inhibition in both acute and chronic studies in Long Evans rats.

phenyl analogues. This was observed not only when comparing cytochrome inhibition, thus removing some concerns about potential for drug−drug interactions, but selectivity was also improved over the homologous nicotinic muscle α1 and ganglionic α3 receptors.

Considering the overall excellent spectrum of activity and selectivity shown, we selected the *para*-fluoro substituted compound **16** for further studies, trying to pre-empt potential problems related to broader metabolism and particularly oxidative activation of unsubstituted compounds like **13**. Indeed, we found that while **13** had medium intrinsic clearance in rat liver microsomes, with a value of 18 μL/min/mg, **16** had a low clearance value (below 5 μL/min/mg), indicating a more favorable elimination profile.[25,26]

Table 4 shows further characterization of compound **16**, both in vitro and in vivo, showing high selectivity also against the α4β2 nicotinic receptor, and a good pharmacokinetic profile with excellent oral absorption, and initial plasma levels in line with the binding affinity. Compared with previously reported compound **2**,[13] **16** displayed improved binding affinity and its increased potency was also confirmed in the electrophysiology experiment. Longer half-life and improved

oral bioavailability were also observed, potentially linked to increased stability of the urea moiety compared to the amide present in compound **2**. A lower brain-to-plasma ratio was measured for **16**, and unfortunately moderate hERG activity was observed, although a level of differentiation over the affinity for the α7 receptor was reached, especially when considering the pharmacokinetic parameters and a protein binding of 75%.[27]

Compound **16** was also characterized in several in vivo behavioral models, displaying efficacy in assays of cognitive function and perceptual processing, showing ability to attenuate pharmacologically induced deficits via the glutamatergic system. Treatment with **16** reversed a (+)-5-methyl-10,11-dihydro-5*H*-dibenzo[*a*,*d*]cyclohepten-5,10-imine (dizocilpine, MK-801) induced deficits in both the novel object recognition memory (Figure 3a) and prepulse inhibition models (Figure 3b) with a minimum efficacious dose of 3 mg/kg in spite of the relatively moderate brain to plasma ratio. Differently from the initial lead **2** where efficacy was observed after ip administration, activity of **16** was observed in both models after oral administration.

Importantly, in the prepulse inhibition test **16** was active both in the acute and in the chronic studies, showing no tolerance to the compound. Although the brain-to-plasma ratio suggests brain exposure levels one order of magnitude lower than the in vitro EC_{50} value (181 ng/mL for the electrophysiology experiment), our results are in line with recent findings that brain levels of agonists required to elicit in vivo effects may lie at the low end of the concentration−response curve defined in vitro using rapid agonist application.[11]

Scheme 1. Synthesis of Aminoalkanoic Acid Amides[a]

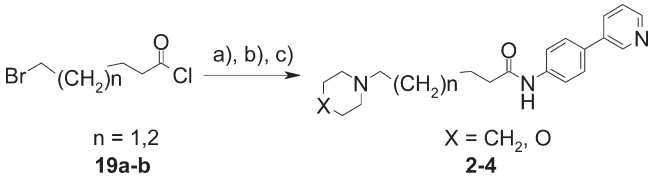

[a] (a) Et_3N, 4-bromoaniline, CH_2Cl_2; (b) piperidine or morpholine, Et_3N; (c) 3-pyridylboronic acid, $Pd(PPh_3)_4$, Na_2CO_3, $MeCN/H_2O$.

Chemistry

The compounds investigated were synthesized using two modifications of the same general route.

The reverse amide compounds were synthesized as already described[13] and shown in Scheme 1 in a one-pot reaction between the appropriate ω-bromoalkanoyl chloride (**19a**,**b**) and 4-bromoaniline, followed by treatment with piperidine or morpholine and Suzuki coupling with 3-pyridylboronic acid.

Ureas **5**−**11** were synthesized using standard methodology, starting from 4-bromophenylisocyanate reaction with aminoalkylamines **20** or **21**, followed by cross-coupling reaction (Scheme 2).

In the case of compound **12**, we failed to obtain the desired product through reaction of **22** with 2-pyridylboronic acid. We therefore reversed the cross-coupling partners after synthesizing boronic esters **24** and **25** as shown in Scheme 3. Boronic ester **25** was then submitted to standard coupling conditions to afford **12**.

For compounds **13**−**18**, where the first ring in the right-hand side system is a pyridine, we activated 6-bromo-pyridin-3-ylamine with triphosgene and reacted the transiently formed isocyanate in situ with amine **20**, as shown in Scheme 4. For large-scale reactions, we found more advantageous to prepare intermediate **26** activating 6-bromo-pyridin-3-ylamine via the more stable isopropenyl carbamate derivative which could be

Scheme 2. Synthesis of Aminoalkyl Phenyl Ureas[a]

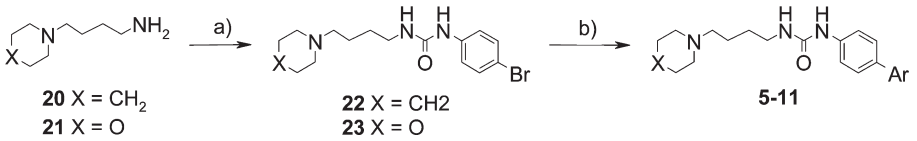

[a] (a) Et_3N, 4-bromophenylisocyanate, CH_2Cl_2; (b) aryl or heteroaryl boronic acid, $Pd(PPh_3)_4$, Na_2CO_3, $MeCN/H_2O$.

Scheme 3. Alternative Route to Aminoalkyl Phenyl Ureas[a]

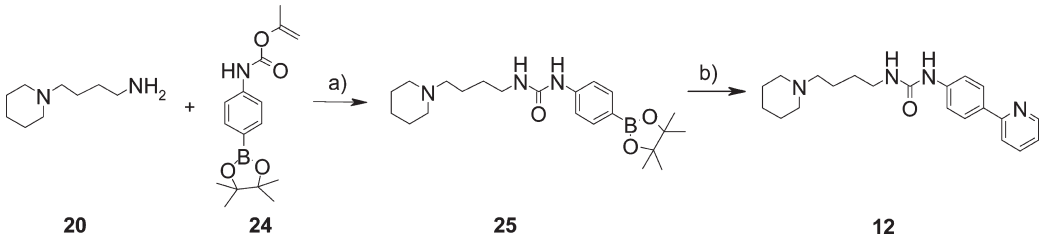

[a] Reagents and conditions: (a) *N*-methylpyrrolidine (cat.), THF, 55 °C; (b) 2-bromopyridine, $Pd(PPh_3)_4$, Na_2CO_3, $MeCN/H_2O$.

Scheme 4. Synthesis of Aminoalkyl Pyridyl Ureas[a]

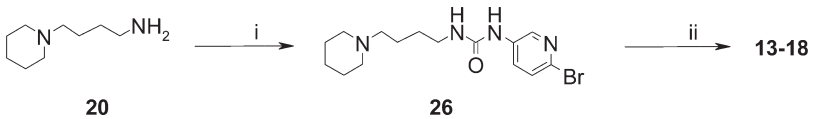

[a] Reagents and conditions: (i) Et_3N, 6-bromo-pyridin-3-ylamine, triphosgene, or isopropenyl chloroformate, CH_2Cl_2; (ii) aryl or heteroaryl boronic acid, $Pd(PPh_3)_4$, Na_2CO_3, $MeCN/H_2O$.

isolated and reacted more conveniently and safely (see Experimental Section).

Conclusions

In summary, we have identified a series of novel derivatives containing a urea moiety, potent agonists of the α7 nAChR with improved profile over the initial lead molecule **2**. In particular, compound **16** (SEN34625/WYE-103914) showed potency, selectivity, and exposures leading to excellent in vivo efficacy and was selected for further exploratory studies. This series is in our opinion of particular interest as it represents further development of a novel structural motif in the nicotinic agonists area compared to the more explored azabicyclic derivatives.[28]

Experimental Section

1. Chemistry. General Methods. Unless otherwise specified, all nuclear magnetic resonance spectra were recorded using a Varian Mercury Plus 400 MHz spectrometer equipped with a PFG ATB broadband probe. HPLC-MS analyses (5 and 10 min methods) were performed with a Waters 2795 separation module equipped with a Waters Micromass ZQ (ES ionization) and Waters PDA 2996, using a Waters XTerra MS C18 3.5 μm 2.1 mm × 50 mm column. Preparative HPLC was run using a Waters 2767 system with a binary gradient module Waters 2525 pump and coupled to a Waters Micromass ZQ (ES) or Waters 2487 DAD, using a Supelco Discovery HS C18 5.0 μm 10 mm × 21.2 mm column. Gradients were run using 0.1% formic acid/water and 0.1% formic acid/acetonitrile with gradient 5/95 to 95/5 with a runtime of 5 or 10 min as stated in the examples. Retention times are expressed in minutes. The purity of compounds submitted for screening were >95% as determined by integrating at 215 nm the peak area of the LC chromatograms. To further support the purity statement, all compounds were also analyzed at a different wavelength (254 nm), and total ion current (TIC) chromatogram and NMR spectra were used to further substantiate results. HRMS data were obtained through (data with five-decimal place precision) a LTQ-Orbitrap mass spectrometer or (data with four-decimal place precision) through an Agilent 6220 TOF, using the manufacturer's MassHunter software, via direct infusion of a 1 μM sample in ACN 30%/FA 0.1% (flow: 5 μL/min). The LTQ-Orbitrap instrument was calibrated prior to analysis with a H_3PO_4 1% solution in mass range 100−800 m/z. Each determination was the combination of 10 successive scans acquired at 60.000 fwhm resolution. For the Agilent 6220 TOF, tuning and calibration parameters were set using the manufacturer's auto tune and auto calibrate solutions and software. Elemental composition calculations were executed using the specific tool included in the QulBrowser module of Xcalibur (Termofisher Scientific, release 2.0.7) software, using a tolerance of 5 ppm. All column chromatography was performed following small modifications of the original method of Still.[29] All TLC analyses were performed on silica gel (Merck 60 F254) and spots revealed by UV visualization at 254 nm and $KMnO_4$ or ninhydrin stain. All microwave reactions were performed in a CEM Discover oven. The Isolute SCX cartridges (1, 2, and 10 g sorbent weight) were purchased from Biotage.

2. Synthesis. General Procedure for Aminoalkylamine Synthesis. To a suspension of the required amine (1 mol equiv), sodium iodide (0.5 mol equiv), and potassium carbonate (1.1 mol equiv) in 2-butanone (4 M solution) *N*-(ω-bromoalkyl) phthalimide (1 mol equiv) was added. The resulting suspension was stirred for 18 h at 85 °C, and then the reaction was filtered and the solvent removed by vacuum distillation; the resulting oil was washed with water and recovered with DCM. The solvent was removed under reduced pressure to yield the amino-phthalimide derivative pure enough to be used in the following step. If necessary, a further purification was carried out by flash-chromatography. The phthalimides thus obtained (1 mol equiv) were dissolved in EtOH to obtain a 2 M solution and hydrazine monohydrate (2 mol equiv) was added dropwise. The mixture was heated at 80 °C for 4 h, after which the reaction was acidified with 37% HCl and the solid which precipitated was removed by filtration. The solution was concentrated under vacuum and taken up with 1N HCl. Any residual 2,3-dihydrophthalazine-1,4-dione was removed by filtration. The aqueous solution was removed under reduced pressure under vacuum to recover the pure product.

4-Piperidin-1-yl-butylamine (20). The general procedure for aminoalkylamine synthesis was followed, starting with piperidine (1.98 mL, 20 mmol). The title product was purified by SCX cartridge eluting with MeOH:DCM 1:1, followed by 2 M NH_3 in MeOH, to obtain 410 mg of compound as a colorless oil (35% yield).

^{1}H NMR (400 MHz, $CDCl_3$): δ (ppm): 1.39−1.62 (m, 9H), 1.91−2.08 (m, 3H), 2.27−2.33 (m, 2H), 2.33−2.44 (m, 3H), 2.71 (t, J = 6.8, 2H). Mass (ES) m/z %: 157 (M + 1, 100%). HPLC: t_R = 0.31, area 100%; (5 min method).

4-Morpholin-4-yl-butylamine (21). The general procedure for aminoalkylamine synthesis was followed, starting from morpholine (2.07 g, 23.8 mmol). The crude was treated with HCl 2 M, the solid was filtered off and the aqueous solution was evaporated to dryness. The residue was taken in isopropanol and filtered to give 3.10 g of solid title compound as hydrochloride salt (67% yield). ^{1}H NMR (400 MHz, $CDCl_3$) δ (ppm): 1.18−1.34 (m, 2H), 1.42−1.57 (m, 4H), 2.35 (t, J = 7.7, 2H), 2.39−2.50 (m, 4H), 2.71 (t, J = 6.2, 2H), 3.68−3.75 (m, 4H).

General Procedure for Urea Synthesis. WARNING: isocyanates and phosgene derivatives (e.g., triphosgene) are highly toxic and should only be handled in a fume hood while wearing appropriate personal protective equipment. To a cooled solution of amine (1 mol equiv) in dichloromethane, the required isocyanate (1 mol equiv) was added. The mixture was left stirring at 0 °C for 1−4 h. The *p*-bromophenyl ureas generally precipitated out of solution as a white solid, recovered by filtration, and if necessary purified further by washing with Et_2O or by flash chromatography.

1-(4-Bromophenyl)-3-(4-piperidin-1-ylbutyl) urea (22). Following the general procedure for urea synthesis, 4-piperidin-1-yl-butylamine (2.34 g, 15.0 mmol) was dissolved in 60 mL of DCM and 4-bromophenylisocyanate (2.97 g, 15.0 mmol) in 15 mL of DCM to give 3.98 g of title compound obtained as a white solid (75% yield) after solvent removal and trituration with Et_2O, which was used without further characterization. ^{1}H NMR (400 MHz, DMSO-d_6): δ 1.40 (m, 10H), 2.19 (m, 2H), 2.26 (m, 4H), 3.05; (m, 2H), 6.16 (s, 1H), 7.35 (m, 4H), 8.52 (s, 1H). Mass (ES) m/z %: 354.30, 356.25 (M + 1, 100%, Br pattern). HPLC t_R = 1.73; area 100% (10 min method)

1-(4-Bromophenyl)-3-(4-morpholin-4-ylbutyl) urea (23). Following the general procedure for urea synthesis and starting from 4-morpholin-4-ylbutylamine (0.72 g, 4.58 mmol), 1.4 g of title compound were obtained as solid by filtration from the reaction solution (86% yield). ^{1}H NMR (400 MHz, $CDCl_3$) δ (ppm): 1.40 (m, 4H), 2.30 (m, 6H), 3.06 (m, 2H), 3.53 (m, 4H), 6.16 (m, 1H), 7.34 (s, 4H), 8.51 (s, 1H).

1-(6-Bromopyridin-3-yl)-3-(4-piperidin-1-ylbutyl)-urea (26). To a solution of 6-bromopyridin-3-ylamine (3.46 g, 20 mmol) in dichloromethane (70 mL), triphosgene (1.96 g, 6.6 mmol) and triethylamine (2.2 g, 22 mmol) were added under N_2 at 0 °C. After 15 min, a solution of 4-piperidin-1-ylbutylamine (3.12 g, 20 mmol) in DCM (10 mL) was added dropwise at 0 °C. The reaction mixture was allowed to warm to room temperature and stirred for 2 h. Dichloromethane was removed in vacuo and the residue dissolved in EtOAc and washed with H_2O. The aqueous layer was basified with solid Na_2CO_3 to pH 9−10 and extracted with EtOAc. The combined organic layers were dried over Na_2SO_4 and evaporated in vacuo to give 5 g of the desired product as a solid (yield: 70%). ^{1}H NMR (400 MHz, $CDCl_3$): δ

1.45−1.62 (m, 8H), 2.29−2.48 (m, 8H), 3.22−3.24 (m, 2H), 6.19 (m, 1H), 7.35 (d, J = 8.7, 1H), 7.54 (bs, 1H), 7.95 (dd, J = 8.7, 2.8, 1H), 8.17 (d, J = 2.8, 1H).

6-Piperidin-1-ylhexanoic acid (4-pyridin-3-yl-phenyl)-amide (4). (a) 6-Piperidin-1-yl-hexanoic acid (4-bromophenyl)-amide: A 0.2 mmol/mL solution of 4-bromoaniline (697 mg, 4.1 mmol) and triethylamine (415 mg, 4.1 mmol) in dichloromethane was cooled at 0 °C under nitrogen atmosphere. A 0.3 mmol/mL solution of 6-bromohexanoyl chloride (**19b**, 869 mg, 4.1 mmol) in dichloromethane was slowly added. The mixture was stirred at room temperature for 1.5 h, after which piperidine (1.74 g, 16.8 mmol) and triethylamine (415 mg, 4.1 mmol) were added. The mixture was stirred at room temperature for 18 h and then at reflux temperature for further 20 h. The mixture was then cooled, the organic solution was washed with brine and dried, and the solvent removed under reduced pressure. Trituration from Et_2O:hexane 1:1 gave 1.02 g of title compound (yield 71%). ^{1}H NMR (400 MHz, DMSO-d_6): δ 1.40 (m, 12H), 2.23 (m, 8H), 7.43 (d, J = 8.9 Hz, 2H,), 7.54 (d, J = 8.9 Hz, 2H), 9.99 (s, 1H). (b) 6-Piperidin-1-yl-hexanoic acid (4-pyridin-3-ylphenyl)-amide: To a degassed mixture of 6-piperidin-1-ylhexanoic acid (4-bromophenyl)amide (120 mg, 0.34 mmol), 3-pyridyl boronic acid (46 mg, 0.37 mmol) in acetonitrile/sodium carbonate 0.4 M solution 1/1 (4 mL), a catalytic amount of $Pd(PPh_3)_4$ (5 mmol %) was added. The reaction mixture was heated at 90 °C for 20 min under microwave irradiation (power set at 150 W) and then again other 20 min. The organic layer was separated and concentrated, and the solvent was removed under reduced pressure to afford the crude product which was purified on a SCX cartridge followed by preparative HPLC column, giving 42 mg of title compound (35% yield) as the formate salt. ^{1}H NMR (400 MHz, DMSO-d_6): δ 1.44 (m, 12H), 2.32 (t, J = 7.4 Hz, 2H), 2.56 (m, 6H), 7.44 (dd, J = 7.9, 4.8 Hz, 1H), 7.66 (d, J = 8.8 Hz, 2H), 7.71 (d, J = 8.8 Hz, 2H), 8.02 (ddd, J = 8.0, 2.1, 1.7 Hz, 1H), 8.25 (s, 1H), 8.51 (dd, J = 4.7, 1.5 Hz, 1H), 8.85 (d, J = 2.0 Hz, 1H), 10.05 (s, 1H). Mass (ES) m/z %: 352 (M + 1, 100%). HPLC t_R = 0.28; area 100%; (10 min method). HRMS: calcd for $C_{22}H_{29}N_3O + H^+$, 352.2383; found (ESI, $[M + H]^+$ obsd), 352.2382.

1-(4-Piperidin-1-yl)butyl-3-(4-pyridin-3-ylphenyl) urea (5). 1-(4-Bromophenyl)-3-(4-(piperidin-1-yl)butyl) urea (3.0 g, 8.45 mmol), pyridine-3-boronic acid (1.76 g, 14.4 mmol), and cesium carbonate (5.51 g, 16.9 mmol) were suspended in 60 mL of toluene and 30 mL of ethanol and the mixture degassed with a nitrogen stream. Tetrakis (triphenylphosphine) palladium (0.29 g, 0.25 mmol) was added and the mixture heated at 85 °C for 15 h. The mixture was then filtered warm on celite and the solvent removed under reduced pressure. HCl 1 M was added and the impurities extracted with EtOAc. The aqueous phase was then basified by NaOH 10% and extracted with DCM. The precipitate formed at the interface was filtered and recrystallized from acetonitrile affording 1.56 g of pure product (yield: 52%).

^{1}H NMR (400 MHz, DMSO-d_6): δ 1.41 (m, 10H), 2.23 (m, 6H), 3.07 (m, 2H), 6.17 (t, J = 5.6 Hz, 1H), 7.42 (dd, J = 8.0, 3.2 Hz, 1H,), 7.50 (d, J = 8.8 Hz, 2H), 7.59 (d, J = 8.8 Hz, 2H), 7.99 (ddd, J = 7.9, 2.4, 1.7 Hz, 1H), 8.48 (dd, J = 4.7, 1.6 Hz, 1H), 8.54 (s, 1H), 8.83 (dd, J = 2.4, 0.7 Hz, 1H). Mass (ES) m/z %: 353 (M + 1, 100%). HPLC: t_R = 0.27; area 100%; (10 min method). HRMS: calcd for $C_{21}H_{28}N_4O + H^+$, 353.23359; found (ESI, $[M + H]^+$ obsd), 353.23357.

1-(4-(Morpholin-4-yl)butyl)-3-(4-pyridin-3-ylphenyl) urea (6). To a degassed solution of 1-(4-bromophenyl)-3-(4-morpholin-4-ylbutyl) urea (82 mg, 0.23 mmol), pyridine-3-boronic acid (37 mg, 0.3 mmol) was added dissolved in acetonitrile/0.4N aqueous Na_2CO_3 1/1 (1 mL/g substrate). After addition of $Pd(PPh_3)_4$ (5−10% mol), the reaction mixture was heated at 90 °C for 20 min under microwave irradiation (power set at 150 W). The acetonitrile layer was separated, the solvent was removed under reduced pressure, and the crude material was purified through a SCX cartridge (eluting with a gradient of DCM/MeOH, followed by MeOH, and finally NH_3/MeOH). The fractions containing the product were combined and dried under reduced pressure. The title compound was obtained in 43% yield (36 mg). ^{1}H NMR (400 MHz, MeOD): δ 1.43 (m, 4H), 2.28 (m, 6H), 3.08 (m, 2H), 3.54 (m, 4H), 6.20 (m, 1H), 7.41 (m, 1H), 7.50 (d, J = 7.4 Hz, 2H), 7.58 (d, J = 8.2 Hz, 2H), 7.99 (d, J = 7.7 Hz, 1H), 8.48 (s, 1H), 8.57 (m, 1H), 8.83 (s, 1H). Mass (ES) m/z %: 355 (M + 1, 100%). HPLC t_R = 0.58; area 100%; (10 min method). HRMS: calcd for $C_{20}H_{26}N_4O_2 + H^+$, 355.2129; found (ESI, $[M + H]^+$ obsd), 355.2125.

1-(4-Piperidin-1-ylbutyl)-3-(4-pyridin-2-ylphenyl) urea (12). (a) 1-(4-Piperidin-1-ylbutyl)-3-[4-(4,4,5,5-tetramethyl-[1,3,2]-dioxaborolan-2-yl)phenyl] urea (**25**): 4-(4,4,5,5-Tetramethyl-1,3,2-dioxaborolan-2-yl)aniline (2.0 g, 9.1 mmol) and *N*-methylmorpholine (1.22 mL, 10.9 mmol) were dissolved in 15 mL of THF, and the resulting solution was cooled down to 0 °C. Isopropenyl chloroformate (1.19 mL, 10.9 mmol) was added dropwise with stirring, and the mixture was allowed to reach ambient temperature and stirred for additional 3 h. The solvent was removed under reduced pressure and the crude product dissolved in DCM, washed twice with 10 mL of brine, and dried over $MgSO_4$. The solution was filtered and the solvent removed under reduced pressure to give [4-(4,4,5,5-tetramethyl-[1,3,2]-dioxaborolan-2-yl)-phenyl]carbamic acid isopropenyl ester **24** as a white powder, which was used in the next step without further purification (2.49 g, yield 90%). A solution of **24** (14.5 mmol) and 4-piperidin-1-ylbutylamine (2.24 g, 14.5 mmol) in THF (5 mL) was heated to 55 °C. To this solution, 1-methylpyrrolidine was added (0.16 mL, 1.45 mmol) and the reaction was stirred at 55 °C for 24 h. Upon reaction completion, as monitored by carbamic ester disappearance (LCMS analysis), the reaction was cooled to room temperature. The solvent and residual reagents were removed under reduced pressure to afford **25** in 92% yield (5.38 g, 13.4 mmol). ^{1}H NMR (400 MHz, $CDCl_3$): 1.32 (m, 12H); 1.55 (m, 10H); 2.37 (m, 6H); 3.25 (s, 2H); 6.80 (s, 1H), 6.55 (s, 1H), 7.30 (d, 2H), 7.75 (d, 2H). Mass (ES) m/z %: 402.23 (M + 1, 100%. HPLC: t_R = 2.20; area 100%; (10 min method). (b) 1-(4-Piperidin-1-yl-butyl)-3-(4-pyridin-2-yl-phenyl)-urea (**12**): A suspension of 2-bromopyridine (31 mg, 0.20 mmol), **25** (96 mg, 0.24 mmol), and $Pd(PPh_3)_4$ (23 mg, 0.02 mmol) in a mixture of 1 mL of sodium carbonate 0.4 M and 1 mL of acetonitrile was stirred at 75 °C for 12 h. The acetonitrile was removed in vacuum and the title compound purified by crystallization from ethyl acetate. Pd traces were removed by dissolving the compound in methanol and passing the solution through a 500 mg PL-Thiol MP SPE (Polymer Laboratories, now part of Varian Inc.) cartridge eluting with methanol. The solvent was evaporated to give 12 mg of the title compound (17% yield). ^{1}H NMR (400 MHz, DMSO): δ 1.33−1.49 (m, 10H), 2.19−2.27 (m, 6H), 3.07−3.09 (m, 2H), 6.25 (t, J = 8.0, 1H), 7.22−7.26 (m, 1H), 7.47−7.49 (m, 2H), 7.77−7.85 (m, 2H), 7.93−7.96 (m, 2H), 8.58−8.59 (m, 1H), 9.57 (bs, 1H). Mass (ES) m/z %: 353 (M + 1, 100%). HPLC: t_R = double peak at solvent front observed at 0.35, 0.84; total area 100% (10 min method). HRMS: calcd for $C_{21}H_{28}N_4O + H^+$, 353.23359; found (ESI, $[M + H]^+$ obsd), 353.23370.

1-[6-(4-Fluorophenyl)pyridin-3-yl]-3-(4-piperidin-1-ylbutyl) urea (16). (a) (6-Bromo-pyridin-3-yl)-carbamic acid isopropenyl ester: To a solution of NaOH (1.13 g, 28.3 mmol) in 56 mL of water, a solution of 6-bromo-pyridin-3-ylamine (3.26 g, 18.8 mmol) in 112 mL of DCM was added. The mixture was cooled at 0 °C, and isopropenyl chloroformate (3.16 g, 26.4 mmol) was added in one hour dissolved in 15 mL of DCM maintaining the solution at 0 °C. The mixture was then allowed to reach room temperature and stirred overnight. The organic phase was separated and evaporated at reduced pressure, maintaining the temperature of the evaporator bath below 25 °C. The crude product obtained was used in the next reaction without further purification. Mass (ES) m/z %: 257−259 (M + 1, 100%, Br pattern). HPLC t_R = 1.88; area 84% (5 min method). 1-(6-Bromopyridin-3-yl)-3-(4-piperidin-1-ylbutyl) urea (**26**): The crude product obtained in the previous reaction was dissolved in 80 mL of THF, and 4-piperidin-1-ylbutylamine

(2.94 g, 18.8 mmol) was added. The solution was refluxed under nitrogen atmosphere for 2.5 h. After evaporation of the solvent, the product was dissolved in DCM. The organic phase was washed with brine, evaporated, and dried to give 6.22 g of title product (yield: 93%). Mass (ES) m/z %: 355−357 (M + 1, 100%, Br pattern). HPLC t_R = 1.08; area 100% (5 min method). (b) 1-[6-(4-Fluorophenyl)pyridin-3-yl]-3-(4-piperidin-1-ylbutyl) urea: 1-(6-Bromopyridin-3-yl)-3-(4-piperidin-1-ylbutyl) urea (6.22 g, 17.5 mmol), 4-fluorophenylboronic acid (3.68 g, 26.3 mmol), and cesium carbonate (11.4 g, 35.0 mmol) were dissolved in 143 mL of toluene and 72 mL of EtOH and the mixture degassed with a nitrogen stream. Tetrakis(triphenylphosphine) palladium (0.61 g, 0.52 mmol) was added and the mixture heated at 90 °C for 2 h. The warm reaction mixture was then filtered on celite and the solvent evaporated. The product was purified by SiO_2 column (gradient from 100% DCM to DCM-2N methanolic ammonia 8:2). The product obtained was crystallized from ethyl acetate, affording 2.14 g (yield: 33%) of the title product. ^{1}H NMR (400 MHz, DMSO): δ 1.31−1.47 (m, 10H), 2.19−2.34 (m, 6H), 3.07−3.09 (m, 2H), 6.31 (t, J = 5.6, 1H), 7.25 (t, J = 8.9, 2H), 7.81 (d, J = 8.7, 1H), 7.95−8.04 (m, 3H), 8.56 (d, J = 2.5, 1H), 8.68 (s, 1H). Mass (ES) m/z %: 371 (M + 1, 100%). HPLC: t_R = 1.75; area 99% (10 min method). HRMS: calcd for $C_{21}H_{27}FN_4O + H^+$ 371.22417; found (ESI, $[M + H]^+$ obsd), 371.22421.

3. Biology. Ca^{2+}-Flux and Membrane Potential Measurements with a Fluorescence Imaging Plate Reader. The following recombinant cell lines were used as specific sources of receptors: GH4C1 cells stably transfected with pCEP4/rat α7 nAChR as previously described,[17] HEK293 cell lines stably expressing human 5-HT_{3A} receptors.[17] Native neuroblastoma SH-SY5Y cells were used as source of human ganglionic nAChRs (α3), and TE671 rhabdomyosarcoma cells were used as endogenous source of muscle $\alpha1\beta1\delta\gamma$ receptors. GH4C1 cells expressing α7 and HEK cells expressing 5-HT_{3A} receptors were analyzed by Ca^{2+}-flux measurements employing a Fluorometric Imaging Plate Reader (FLIPR, Molecular Devices) system, whereas the cells expressing the nicotinic receptor subunits α1 and α3 were tested in the FLIPR system with a membrane potential sensitive dye. For Ca^{2+}-flux analysis, cells were plated in 96-well clear-bottom, poly D-lysine coated black microtiter plates (Costar) at a density of 1×10^5 cells/well for α7 expressing GH4C1 cells or 8×10^4 cells/well for 5-HT_{3A} expressing HEK293 cells and cultured for 24 h prior to experiments. The medium was then replaced with 100 μL of Hank's Balanced Salt Solution-HEPES 20 mM, pH 7.4 (assay buffer) containing 4 μM Fluo-4-AM, 0.02% pluronic acid, and 5 mM probenecid. After 40 min of incubation at 37 °C, the labeling solution was replaced with 200 μL of assay buffer containing 2.5 mM probenecid. Plates were then transferred to the FLIPR system. Compounds to be tested were prepared in assay buffer as 5×-concentrated solutions in a separate 96-well polypropylene plate. Basal fluorescence was recorded for 30 s, followed by addition of 50 μL of test compound (to assess agonist activity; first addition). Measurements were made at 1 s intervals for 1 min, followed by measurements every 30 s for 10 min. Subsequently, for the second addition for alpha-7 expressing GH4C1 cells, nicotine was added to each well except negative controls at EC_{80} final concentration to assess antagonism of nicotine response or at EC_{20} final concentration to assess positive modulation of nicotine response. Assay performance was robust as reflected by a Z' factor > 0.6.

For testing 5-HT_{3A} receptor activity, *m*-chlorophenylbiguanide (CPBG, EC_{80} final concentration) was added to each well except negative controls. Measurements were made at 1 s intervals for 1 min after the second addition and at 3 s intervals for the remaining 3 min. Results were exported from the FLIPR raw data as MAX-MIN of fluorescence signal intensity in two intervals corresponding to the first and the second addition of compounds. The responses were normalized to the positive control and EC_{50} and IC_{50} values were calculated using XlFit version 4.2, with a sigmoidal concentration−response (variable slope) equation: Y = Bottom + (Top − Bottom)/(1 + $(EC_{50}/X)^{\text{Hill Slope}}$), where X is the concentration, Y is the response, Bottom is the bottom plateau of the curve, and Top the top plateau.

Activity of compounds at the muscle and ganglionic type nAChR receptors was determined using a membrane potential sensitive fluorescent dye. TE671 and SHSY5Y cells were plated at a density of 5×10^4 and 1×10^5 cells/well, respectively, 24 h prior to assay. Growth media were removed from the cells by flicking the plates, and membrane potential dye (Molecular Devices), reconstituted in HBSS five times more diluted compared to the manufacturer's instructions, was added to the wells. Plates were incubated for 60 min at room temperature and then directly transferred to the FLIPR system. Compounds to be tested were prepared in assay buffer as 5×-concentrated solutions in a separate 96-well polypropylene plate. Baseline fluorescence was monitored for the first 10 s followed by the addition of compounds. For detection of antagonists activity, agonist (epibatidine; EC_{80} final concentration) was added to every well except negative controls. Signal recordings were performed as above. Results were exported from the FLIPR raw data as SUM of fluorescence signal intensity for the first addition and MAX−MIN for the second addition of compounds. The responses were normalized to the positive control (epibatidine 1 μM final concentration). The compounds tested were found to display antagonist activity, and IC_{50} values were calculated as described before.

Solubility Assay. Standard and sample solutions were prepared from a 10 mM DMSO stock solution using an automated dilution procedure. For each compound, three solutions were prepared; one to be used as standard and the other two as test solutions. Standard: 250 μM standard solution in acetonitrile/buffer, with a final DMSO content of 2.5% (v/v). Test sample for pH 3.0: 250 μM sample solution in acetic acid 50 mM, pH = 3, with a final DMSO content of 2.5% (v/v). Test sample for pH 7.4: a 250 μM sample solution in ammonium acetate buffer 50 mM, pH = 7.4, with a final DMSO content of 2.5% (v/v). The 250 μM product suspensions/solutions in the aqueous buffers were prepared directly in Millipore MultiScreen-96 filter plates (0.4 μm PTCE membrane) and sealed. Plates were left for 24 h at room temperature under orbital shaking to achieve "pseudo-thermodynamic equilibrium" and to presaturate the membrane filter. Product suspensions/solutions were then filtered using centrifugation, diluted 1:2 with the same buffer solution, and analyzed by UPLC/UV/TOF-MS, using UV-detection at 254 nm for quantitation. Solubility was calculated by comparing the sample and standard UV areas: $S = (A_{smp} \times F_D \times C_{st})/A_{st}$, where S is the solubility of the compound (μM), A_{smp} is the UV area of the sample solution, F_D is the dilution factor (2), C_{st} is the standard concentration (250 μM), and A_{st} is the UV area of the standard solution.

Cytochrome Inhibition Assay.[23,30] The fluorescent P450 inhibition assay was performed using the Gentest method (http://www.gentest.com). Test compounds were dissolved in DMSO at 1.5 mM. The stock solution of 12 μL was added by a robotic system to 1488 μL of 0.1 M phosphate buffer at pH 7.4. The solution was mixed, and 50 μL of the diluted samples was added to a 1 mL 96-well polypropylene plate. Then 50 μL of cofactor with NADPH regenerating system were added to the wells. The plate was incubated at 37 °C for at 10 min. Enzyme−substrate mix was prepared by prewarming the buffer at 37 °C for at least 10 min, and the enzymes and substrates were added right before addition to the reaction plate. Enzyme−substrate mix (100 μL) was added to the wells to start the reaction. The final substrate and isozyme concentrations and incubation time were: BFC (50 μM)/CYP3A4 (5 pmol/mL) for 30 min, AMMC (1.5 μM)/CYP2D6 (7.5 pmol/mL) for 30 min, and MFC (75 μM)/2C9 (20 pmol/mL) for 45 min. The reactions were stopped with 80% ACN/20% 0.5 M Tris buffer. The signals were quantified using a fluorescent plate reader. The final DMSO concentration was

0.2%. Compounds were tested in duplicates. Percent inhibition was determined at 3 μM compound concentration. High negative values are usually indicative of fluorescent interference from the test compounds or metabolites. The % CV obtained was typically within 10%.

Metabolic Stability Assay. Compounds in 10 mM DMSO solution were added to an incubation mixture in a 96-well microplate containing 20 pmol/mL of hCYP3A4 (0.1−0.2 mg/mL protein). The mixture was split in two aliquots: one receiving a NADPH regenerating system, the other an equal amount of phosphate buffer. The final substrate concentration was 1 μM along with 0.25% of organic solvent. Incubation proceeded for 1 h at 37 °C and was stopped by addition of acetonitrile to precipitate proteins. Metabolic stability is given as the percent remaining following incubation with cofactor (NADPH) with reference to the incubation mixture without NADPH: % remaining = Area NADPH × 100/Area ctrl where Area ctrl is the MS peak area of the sample solution without NADPH and AreaNADPH is the MS area of the sample solution with NADPH. The % CV obtained was typically within 10%.

Permeability Assay. The assay was run in a PAMPA filter plate, and compounds (10 μM in HBSS + Hepes buffer) were added to the donor chamber and incubated for 4 h at 37 °C and 80% humidity. Warfarin was used as reference control. Concentrations of reference, donor, and acceptor solutions were measured by UPLC-MS-TOF (references, donor, and acceptor were injected in UPLC-MS in this order to compare the MS quantitative signal).

The passive permeability is calculated according to a modified version of the following expression[31]

$$CAA(t) = \left(\frac{M}{V_D + V_A}\right) + \left(Ca(0) - \frac{M}{V_D + V_A}\right)e - P_e A\left(\frac{1}{V_D} + \frac{1}{V_A}\right)t$$

where M refers to total amount of drug in the system minus the amount of sample lost in membrane (and surfaces), $CA(t)$ is the concentration of the drug in the acceptor well at time t, $CA(0)$ is the concentration of the drug in the acceptor well at time 0, V_A is the volume of the acceptor well, V_D is the volume of the donor well, P_e is the effective permeability, A is the membrane area, and t is the permeation time. Compounds are defined as low, medium, or highly permeable following the following classification: $> 10 \times 10^{-6}$ cm/s, high (passive permeability is unlikely to be limiting for passive diffusion); between 2 and 10×10^{-6} cm/s, medium (permeability may be limiting in case of low solubility, high metabolic turnover rate or active secretion); between 0 and 2×10^{-6} cm/s, Low (high risk that permeability is limiting for passive diffusion).

Rat Microsomal Stability. DMSO stock solutions of test compounds were prepared at 0.5 mM concentration. Diluted solutions of test compounds were prepared by adding 50 μL of each DMSO stock solution to 200 μL of acetonitrile to make 0.1 mM solutions in 20% DMSO/80% acetonitrile. Rat liver microsomal solution was prepared by adding 1.58 mL of concentrated rat liver microsomes (20 mg/mL protein concentration) to 48.29 mL of prewarmed (to 37 °C) 0.1 M potassium phosphate buffer (pH 7.4) containing 127 μL of 0.5 M EDTA to make a 0.633 mg/mL (protein) microsomal solution. Then 11.2 μL of each test compound diluted solution was each added directly to 885 μL of rat liver microsomal solution (allowing direct binding of drugs to microsomal proteins and lipids to minimize precipitation and nonspecific binding to the plasticware). This solution was mixed, and 180 μL was transferred to time 0 and time 15 min plates (each in duplicate wells). For the time 15 min plate, NADPH regenerating agent (45 μL) was added to each well to initiate the reaction, the plate was incubated at 37 °C for 15 min, followed by quenching of the reaction by adding 450 μL of cold acetonitrile to each well. For the time 0 plate, 450 μL of cold acetonitrile was added to each well, followed by addition of NADPH regenerating agent (45 μL) and no incubation. All of the plates were centrifuged at 3000 rpm for 15 min, and the supernatants were transferred to other well plates for analysis by LC−MS.[25,26]

Electrophysiology. GH4C1 cells stably expressing rat α7-nAChR were treated with 0.5 mM sodium butyrate added to the medium for two days before patch clamp recordings. Patch pipettes had resistances of ∼7 MΩ when filled with (in mM): 5 EGTA, 120 K-gluconate, 5 KCl, 10 HEPES, 5 K_2ATP, 5 Na_2-phosphocreatine, 1 $CaCl_2$, and 2 $MgCl_2$. Cells were voltage-clamped at −60 mV with a HEKA EPC-9 amplifier. To measure the fast activation and desensitization of α7 current, the Dynaflow (Cellectricon) fast perfusion system with 16- or 48-well chips was used. Different concentrations of acetylcholine or **16** were applied to cells in between washes with bath solution (Hanks' Balanced Salt Solution + 10 mM HEPES). Data were acquired at 1 kHz for 2 s episodes (500 ms bath, 500 ms agonist, 1000 ms wash) with a 10 s interval between episodes. Peak current amplitude and total charge (area under the curve) were measured with the HEKA Pulse program. Concentration−response curves and EC_{50} values were plotted and calculated with Origin (MicroCal).

Radioligand Binding Assay. [^{3}H]-Epibatidine binding studies were performed as previously described.[17] Briefly, cell membrane preparations derived from GH4C1 cells stably expressing rat α7 nAChRs were suspended in binding buffer (50 mM HEPES, pH 7.4, 3 mM KCl, 70 mM NaCl, 10 mM $MgCl_2$), 5 nM [^{3}H]-epibatidine (GE Healthcare; SA = 53 Ci/mmol) and **16** to achieve a final volume of 200 μL in a 96-well polypropylene plate. Nicotine at 300 μM was used for determination of nonspecific binding. Following incubation at room temperature (23 °C) for 1 h, samples were rapidly filtered through Unifilter GF/B filters using a Filtermate (Perkin-Elmer) and washed five times with ice-cold binding buffer. Samples were processed and counted for radioactivity using a TopCount NXT (Perkin-Elmer). Competition binding curves were fitted with a four parameter logistic model. K_i values were calculated by the Cheng−Prusoff equation using the GraphPad Prism software package.

Receptor Selectivity and hERG Activity. Interaction of **16** with ∼70 binding sites including all major classes of neurotransmitter, growth factor, and peptide receptors (Novascreen, Caliper Biosciences, Hopkinton MA) was examined at 10 μM concentration. Detectable activity was only observed for $5HT_4$ (K_i = 6 μM): adrenergic α-2A, (IC_{50} = 7.5 μM), adrenergic α-2b (IC_{50} = 35 μM). Activity at hERG ion channel was determined employing CHO cells stably expressing the channel and an IonWorks recording system.

Pharmacokinetics. Long Evans rats (age of 6−8 weeks, body weight 250−550 g) were administered compound **16** as a single dose of 3 mg/kg po at time 0 as a solution in 2% Tween, 0.5% methocell in water (volume 2.5 mL/kg). Levels in plasma were determined over a time period of 6 h in the po study and in plasma and brain at 0, 0.5, 1, and 3 h. Concentration of **16** in rat brain and plasma was measured by high performance liquid chromatography in combination with mass spectrometry (LC-MS/MS) with a limit of detection of 1 ng/mL in plasma and 10 ng/g in brain. Plasma samples were prepared by protein precipitation with acetonitrile containing 250 ng/mL of internal standard, centrifugation, and analysis of the supernatant by LC-MS/MS. Brain samples were prepared by homogenization and extraction with methanol. The homogenates were subsequently centrifuged, and the supernatant was analyzed by LC-MS/MS. Quantification was performed in a similar manner to the plasma samples.

Object Recognition Test. Male Long Evans rats (ca. 250 g) were individually housed with ad lib access to food and water and provided with nestlets for environmental enrichment. All habituation, training, and testing was performed under low illumination (approximately 10 lx) in a circular arena (70 cm diameter, 30 cm height) constructed of plastic surrounded by a black mesh curtain and containing corncob bedding. Fecal pellets were removed and bedding mixed after each trial. The novel object recognition (NOR) task is composed of three

sessions: habituation, a sample trial, and a choice trial. During habituation, rats were placed into the arena in the presence of two identical yellow blocks (constructed with Duplos plastic blocks) and allowed to explore freely for 10 min. On the following day, the sample trial was initiated in which the animals were returned to the arena for 5 min exposure to two identical stimuli (objects constructed of Duplos) located at opposing compass points approximately 10 cm in from the walls of the arena. After a predefined interval of time, the choice trial was initiated in which animals were again returned to the arena for 5 min, this time with one familiar stimulus (the object the animal was exposed to during the sample trial) and one novel stimulus. To evaluate the effect of **16** in the MK-801-induced deficit model of NOR, the choice trial was carried out 1 h after the sample trial, and animals were treated with vehicle or **16** (0.3−30 mg/kg, po) 60 min prior to the sample trial plus vehicle or MK-801 (0.03 mg/kg, ip) 30 min prior to the sample trial ($N = 10$ per treatment group).

Antagonism of MK-801 Induced Prepulse Inhibition Deficits in Rats. Each testing chamber (SR-LAB system, San Diego Instruments, San Diego, CA) consisted of a Plexiglas cylinder (8.8 cm in diameter) mounted on a frame and held in position by four metal pins to a base unit. Movement of the subjects (male Long Evans rats, 200−300 g, $n = 8$ per treatment group) within the cylinder was detected by a piezoelectric accelerometer attached below the frame. A loudspeaker mounted 24 cm above the cylinder provided background white noise, acoustic noise bursts, and acoustic prepulses. The entire apparatus was housed in a ventilated enclosure (39 cm × 38 cm × 56 cm). Presentation of acoustic pulse and prepulse stimuli were controlled by the SR-LAB software and interface system, which also digitized, rectified, and recorded the responses from the accelerometer. Mean startle amplitude was determined by averaging 100, 1 ms readings taken from the beginning of the pulse stimulus onset. For calibration purposes, sound levels were measured with a Quest sound level meter, scale "A", with the microphone placed inside the Plexiglas cylinder. Test sessions consisted of 61 total trials with a 15 s intertrial interval. Following a 5 min acclimation to a 64 dB background noise, four trial types (20 ms 120 dB pulse, or a 69, 74, or 79 dB 20 ms prepulse paired with a 120 dB 20 ms pulse, occurring 100 ms later onset to onset) were presented in a pseudorandom order. Compound **16** (1−30 mg/kg) was administered orally at 60 min prior to testing with MK-801 (0.085 mg/kg) administered sc 10 min prior to testing. Tolerance was assessed in rats treated chronically with compound **16** (3 mg/kg po per day for 14 days) prior to the experiment. Prepulse inhibition was defined as 100 − [(startle amplitude on prepulse trials/startle amplitude on pulse alone trials) × 100].

4. Modeling Studies. All molecular modeling studies were performed on a DELL PowerEdge server equipped with 4 processors Intel Xeon CPU 3.00 GHz. A homology model of the EC domain of nAChR was built by modeling the human α7 sequence for α7 nAChR on 1UW6 PDB structure as a template (manuscript in preparation). The model was then used for docking purposes.. Compound structures were modeled within Maestro software suite (Maestro version 9.0; Schrodinger, LLC: New York). In particular, ligands were protonated at pH 7.4 and their geometries optimized using LigPrep module (LigPrep 2.3; Schrodinger, LLC: New York).

Docking into the orthosteric binding site of the homology model was performed by the docking program GOLD version 3.0.[32] Ligands were docked using default accurate genetic algorithm settings and the GOLDCORE fitness function. The goodness of the docked poses was mainly evaluated via visual inspection and supported by the scoring value. Key pharmacophoric interaction between protonated nitrogen on the ligand and the backbone carbonyl of W143 was considered as a fundamental requisite to validate docking poses.

Acknowledgment. We thank Eva Genesio for her support in the interpretation of analytical data, Gian Luca Sardone and Stefano Gotta for generation of HRMS, Martina Pollastrini and Laura Bettinetti, for the synthesis of previously reported compounds and Silvia Papini for in vitro testing of some of the reported compounds, and Nicola Caradonna for useful discussions on the pharmacokinetics data.

Supporting Information Available: Experimental details for compounds **7**−**11**, **13**−**15**, **17**−**18** and FLIPR functional data assessing compound **16** in 'positive modulator' assay mode in comparison with data obtained for reported positive modulator PNU120596. This material is available free of charge via the Internet at http://pubs.acs.org.

References

(1) Lindstrom, J. Neuronal nicotinic acetylcholine receptors. *Ion Channels* **1996**, *4*, 377–450.
(2) Newhouse, P.; Singh, A.; Potter, A. Nicotine and Nicotinic Receptor Involvement in Neuropsychiatric Disorders. *Curr. Top. Med. Chem.* **2004**, *4*, 267–282.
(3) Taly, A.; Corringer, P.-J.; Guedin, D.; Lestage, P.; Changeux, J.-P. Nicotinic receptors: allosteric transitions and therapeutic targets in the nervous system. *Nat. Rev. Drug Discovery* **2009**, *8*, 733–750.
(4) Decker, M. W.; Gopalakrishnan, M.; Meyer, M. D. The potential of neuronal nicotinic acetylcholine receptor agonists for treating CNS conditions. *Expert Opin. Drug Discovery* **2008**, *3*, 1027–1040.
(5) Gotti, C.; Riganti, L.; Vailati, S.; Clementi, F. Brain Neuronal Nicotinic Receptors as New Targets for Drug Discovery. *Curr. Pharm. Des.* **2006**, *12*, 407–428.
(6) Acker, B. A.; Jacobsen, E. J.; Rogers, B. N.; Wishka, D. G.; Reitz, S. C.; Piotrowski, D. W.; Myers, J. K.; Wolfe, M. L.; Groppi, V. E.; Thornburgh, B. A.; Tinholt, P. M.; Walters, R. R.; Olson, B. A.; Fitzgerald, L.; Staton, T. J.; Raub, T. J.; Krause, M.; Li, K. S.; Hoffman, W. E.; Hajos, M.; Hurst, R. S.; Walker, D. P. Discovery of *N*-[(3*R*,5*R*)-1-azabicyclo[3.2.1]oct-3-yl]furo[2,3-*c*]pyridine-5-carboxamide as an agonist of the alpha7 nicotinic acetylcholine receptor: in vitro and in vivo activity. *Bioorg. Med. Chem. Lett.* **2008**, *18*, 3611–3615.
(7) Pichat, P.; Bergis, O. E.; Terranova, J.-P.; Urani, A.; Duarte, C.; Santucci, V.; Gueudet, C.; Voltz, C.; Steinberg, R.; Stemmelin, J.; Oury-Donat, F.; Avenet, P.; Griebel, G.; Scatton, B. SSR180711, a novel selective alpha7 nicotinic receptor partial agonist: (II) efficacy in experimental models predictive of activity against cognitive symptoms of schizophrenia. *Neuropsychopharmacology* **2007**, *32*, 17–34.
(8) Lippiello, P. M.; Bencherif, M.; Hauser, T. A.; Jordan, K. G.; Letchworth, S. R.; Mazurov, A. A. Nicotinic receptors as targets for therapeutic discovery. *Expert Opin. Drug Discovery* **2007**, *2*, 1185–1203.
(9) Freedman, R.; Adams, C. E.; Leonard, S. The alpha7-nicotinic acetylcholine receptor and the pathology of hippocampal interneurons in schizophrenia. *J. Chem. Neuroanat.* **2000**, *20*, 299–306.
(10) Kem, W. R. The brain alpha7 nicotinic receptor may be an important therapeutic target for the treatment of Alzheimer's disease: studies with DMXBA (GTS-21). *Behav. Brain Res.* **2000**, *113*, 169–181.
(11) Tietje, K. R.; Anderson, D. J.; Bitner, R. S.; Blomme, E. A.; Brackemeyer, P. J.; Briggs, C. A.; Browman, K. E.; Bury, D.; Curzon, P.; Drescher, K. U.; Frost, J. M.; Fryer, R. M.; Fox, G. B.; Gronlien, J.; Hakerud, M.; Gubbins, E. J.; Halm, S.; Harris, R.; Helfrich, R. J.; Kohlhaas, K. L.; Law, D.; Malysz, J.; Marsh, K. C.; Martin, R. L.; Meyer, M. D.; Molesky, A. L.; Nikkel, A. L.; Otte, S.; Pan, L.; Puttfarcken, P. S.; Radek, R. J.; Robb, H. M.; Spies, E.; Thorin-Hagene, K.; Waring, J. F.; Ween, H.; Xu, H.; Gopalakrishnan, M.; Bunnelle, W. H. Preclinical Characterization of A-582941: A Novel α7 Neuronal Nicotinic Receptor Agonist with Broad Spectrum Cognition-Enhancing Properties. *CNS Neurosci. Ther.* **2008**, *14*, 65–82.
(12) Gaviraghi, G.; Ghiron, C.; Bothmann, H.; Roncarati, R.; Terstappen, G. C. Modulators of alpha7 nicotinic acetylcholine receptors and therapeutic uses thereof. PCT Int. Appl. WO2006008133A2, **2006**.
(13) Haydar, S. N.; Ghiron, C.; Bettinetti, L.; Bothmann, H.; Comery, T. A.; Dunlop, J.; La Rosa, S.; Micco, I.; Pollastrini, M.; Quinn, J.; Roncarati, R.; Scali, C.; Valacchi, M.; Varrone, M.; Zanaletti, R. SAR and biological evaluation of SEN12333/WAY-317538: novel alpha 7 nicotinic acetylcholine receptor agonist. *Bioorg. Med. Chem.* **2009**, *17*, 5247–5258.
(14) Roncarati, R.; Scali, C.; Comery, T. A.; Grauer, S. M.; Aschmies, S.; Bothmann, H.; Jow, B.; Kowal, D.; Gianfriddo, M.; Kelley, C.;

Zanelli, U.; Ghiron, C.; Haydar, S.; Dunlop, J.; Terstappen. Procognitive and neuroprotective activity of a novel alpha7 nicotinic acetylcholine receptor agonist for treatment of neurodegenerative and cognitive disorders. *J. Pharmacol. Exp. Ther.* **2009**, *329*, 459–468.
(15) Xiu, X.; Puskar, N. L.; Shanata, J. A. P.; Lester, H. A.; Dougherty, D. A. Nicotine Binding to Brain Receptors Requires a Strong Cation−π Interaction. *Nature* **2009**, *458*, 534–537.
(16) Compounds **2** and **3** were previously reported in ref 13.
(17) Dunlop, J; Roncarati, R; Jow, B; Bothmann, H; Lock, T; Kowal, D; Bowlby, M; Terstappen, G. C. In vitro screening strategies for nicotinic receptor ligands. *Biochem. Pharmacol.* **2007**, *74*, 1172–1181.
(18) Karlin, A.; Akabas, M. H. Towards a structural basis for the function of nicotinic acetylcholine recetors and their cousins. *Neuron* **1995**, *15*, 1231–1244.
(19) Brejc, K.; van Dijk, W. J.; Klaassen, R. V.; Schuurmans, M.; van Der Oost, J.; Smit, A. B.; Sixma, T. K. Crystal structure of an ACh-binding protein reveals the ligand-binding domain of nicotinic receptors. *Nature* **2001**, *411*, 269–276.
(20) Lester, H. A.; Dibas, M. I.; Dahan, D. S.; Leite, J. F.; Dougherty, D. A. Cys-loop receptors: new twists and turns. *Trends Neurosci.* **2004**, *27*, 329–336.
(21) Feng, M. R. Assessment of blood−brain barrier penetration: in silico, in vitro and in vivo. *Curr. Drug Metab.* **2002**, *3*, 647–657.
(22) Di, L.; Kerns, E.; Fan, K.; McConnell, O. J.; Carter, G. T. High throughput artificial membrane permeability assay for blood−brain barrier. *Eur. J. Med. Chem.* **2003**, *38*, 223–232.
(23) Di, L.; Kerns, E.; Li, S.; Carter, G. Comparison of cytochrome P450 inhibition assays for drug discovery using human liver microsomes with LC−MS, rhCYP450 isozymes with fluorescence, and double cocktail with LC−MS. *Int. J. Pharm.* **2007**, *335*, 1–11.
(24) Smith, D. A.; Jones, B. C.; Walker, D. K. Design of drugs involving the concepts and theories of drug metabolism and pharmacokinetics. *Med. Res. Rev.* **1996**, *16*, 243–266.
(25) Di, L.; Kerns, E.; Li, S.; Petusky, S. High Throughput Microsomal Stability Assay for Insoluble Compounds. *Int. J. Pharm.* **2006**, *317*, 54–60.
(26) Di, L.; Kerns, E.; Ma, X.; Huang, Y.; Carter, G. Applications of high throughput microsomal stability assay in drug discovery. *Comb. Chem. High Throughput Screening* **2008**, *11* (6), 469–476.
(27) Yao, X.; Anderson, D. L.; Ross, S. A.; Lang, D. G.; Desai, B. Z.; Cooper, D. C.; Wheelan, P.; McIntyre, M. S.; Bergquist, M. L.; MacKenzie, K. I.; Becherer, J. D.; Hashim, M. A. Predicting QT prolongation in humans during early drug development using hERG inhibition and an anaesthetized guinea-pig model. *Br. J. Pharmacol.* **2008**, *154*, 1446–1456.
(28) Horenstein, N. A.; Leonik, F. M.; Papke, R. L. Multiple pharmacophores for the selective activation of nicotinic α7-type acetylcholine receptors. *Mol. Pharmacol.* **2008**, *74*, 1496–1511.
(29) Still, W. C.; Kahn, M.; Mitra, A. J. Rapid chromatographic technique for preparative separations with moderate resolution. *J. Org. Chem.* **1978**, *43*, 2923–2925.
(30) Crespi, C. L.; Miller, V. P.; Penman, B. W. Microtiter Plate Assays for Inhibition of Human, Drug-Metabolizing Cytochromes P450. *Anal. Biochem.* **1997**, *248*, 188–190.
(31) Palm, K.; Luthman, K.; Ros, J.; Grasjö, J.; Artursson, P. Effect of Molecular Charge on Intestinal Epithelial Drug Transport: pH-Dependent Transport of Cationic Drugs. *J. Pharmacol. Exp.Ther.* **1999**, *291*, 435–443.
(32) Jones, G.; Willett, P.; Glen, R. C.; Leach, A. R.; Taylor, R. Development and Validation of a Genetic Algorithm for Flexible Docking. *J. Mol. Biol.* **1997**, *267*, 727–748.